

# Exploring the advantages of artificial neural networks in predicting children's thermal perception and their potential application

Xiaoyun He <sup>a,b,c,\*</sup>, Kerry A. Nice <sup>c</sup>, Yuexing Tang <sup>a,b</sup>, Long Shao <sup>a,b</sup>

<sup>a</sup> School of Architecture and Design, Harbin Institute of Technology, Harbin 150001, China

<sup>b</sup> Key Laboratory of Cold Region Urban and Rural Human Settlement Environment Science and Technology, Ministry of Industry and Information Technology, Harbin 150001, China

<sup>c</sup> Transport, Health and Urban Systems Research Lab, Faculty of Architecture, Building, and Planning, the University of Melbourne, Parkville, VIC 3010, Australia

## ARTICLE INFO

### Keywords:

Thermal sensation vote (TSV)  
Children  
Artificial neural network (ANN)  
Predictive model  
Urban park

## ABSTRACT

While numerous thermal comfort models have been developed to predict human thermal comfort levels in outdoor areas under varying weather conditions, these indexes are generally designed for adults. To assess the suitability of thermal comfort models, the Universal Thermal Climate Index and a multiple linear regression (MLR) model based on Predicted Mean Vote factors, to predict children's outdoor thermal sensation votes (TSV), field investigations were conducted in a Harbin park across multiple seasons. In addition, two new artificial neural network (ANN) models, with single and double hidden layers, were developed and validated to address a wider range of input parameters than the traditional models, clothing levels and metabolic rates, as well as accounting for a wider range of ages, body weights and heights. The results demonstrated that: 1) the ANN models outperformed the traditional models; 2) The two-hidden-layer ANN model slightly outperformed the one-hidden-layer model; 3) sensitivity analysis identified the top four parameters influencing the prediction of children's TSV in Harbin as mean radiant temperature (0.259), air temperature (0.200), globe temperature (0.161), and children's metabolic rate (0.110). These findings will offer valuable insights for optimizing thermal environments in urban parks, reducing children's thermal stress, and advancing intelligent park services.

## 1. Introduction

Climate change is impacting human health and well-being, with children being particularly vulnerable to its effects (Z. Xu et al., 2012). As economic and social development progresses, there is a widespread pursuit of more comfortable living conditions, and children have the right to enjoy both comfortable indoor and outdoor environments. However, discussions on climate change often overlook its impact on children (Currie and Deschênes, 2016). According to the World Health Organization (WHO), children's health is currently facing a range of new threats. Adverse outdoor environments directly or indirectly affect children's health (WHO, 2020a).

Outdoor spaces are essential for production, construction, exercise, recreation, and socializing, making them closely intertwined with daily life. Urban parks, as crucial outdoor spaces for residents, play a significant role in influencing physical and mental health

\* Corresponding author at: School of Architecture and Design, Harbin Institute of Technology, Harbin 150001, China.  
E-mail address: [21b934029@stu.hit.edu.cn](mailto:21b934029@stu.hit.edu.cn) (X. He).

(Dadvand et al., 2016; Javadi and Nasrollahi, 2021; Maas et al., 2009; Seltenerich, 2015; Tyrväinen et al., 2014; Vanaken and Danckaerts, 2018; WHO, 2020b). They provide excellent venues for children to participate in outdoor leisure, recreation, and physical activities.

Outdoor thermal comfort is the most significant environmental factor influencing citizens' outdoor activities (Lai et al., 2014a; Qin et al., 2021), and a safe and comfortable outdoor thermal environment also helps minimize the environmental health risks faced by children (Kennedy et al., 2021). Therefore, understanding the thermal perception and comfort of children holds crucial value for enhancing urban outdoor environments (Coccolo et al., 2016). Researchers have established the relationship between the thermal environment and thermal perception by using thermal comfort indices such as Predicted Mean Vote (PMV), Physiologically Equivalent Temperature (PET), and Universal Thermal Climate Index (UTCI), which are then linked to thermal comfort assessment (Chan and Chau, 2019). While thermal perception might not be the ideal concept for gauging satisfaction with the thermal environment, it is frequently employed as an indicator for assessing thermal comfort (Shahzad et al., 2018; von Grabe, 2016).

Currently, there are two common methods for predicting outdoor thermal perception. One method involves using empirical thermal sensation models, specifically employing multiple linear regression (MLR), where outdoor thermal perception is defined as a function of meteorological parameters such as air temperature ( $T_a$ ), wind speed (V), solar radiation (G), and absolute humidity (Cheng et al., 2012; Hadianpour et al., 2018; Lai et al., 2014b; W. Yang et al., 2013; Zhao et al., 2016). This method treats the complex causal relationships between thermal perception and its influencing factors as a black box, simplifying the prediction of thermal sensation. However, although microclimate parameters indeed significantly influence thermal perception, they can only explain around 50 % of the actual variations in respondents' thermal sensation (Nikolopoulou and Steemers, 2003). The other method involves predicting thermal perception through thermal indices. To date, 165 human thermal indices have been developed for assessing thermal comfort and heat stress in hot environments (de Freitas and Grigorieva, 2017). PMV, PET, and UTCI are three widely used indices in outdoor thermal comfort research. Among them, PMV is based on the steady-state heat balance model proposed by Fanger in the 1970s (Fanger, 1970). However, while the PMV model is effective for predicting thermal sensation in static and air-conditioned buildings, its performance is poor for naturally ventilated buildings (Chai et al., 2020) and even worse in dynamic outdoor environments. PET and UTCI are considered reasonable indicators for predicting outdoor thermal comfort and thermal stress, they have been used by some studies as methods to approximate children's thermal comfort and thermal stress (He et al., 2023; Huang et al., 2021; Lam et al., 2021; Shao et al., 2022). However, these indices have certain limitations. While they provide an objective assessment of the thermal environment's impact on the body's thermal state, they do not account for personal factors such as clothing insulation and activity level, which are either excluded or standardized to specific reference values. PET adopts standardized clothing (0.9 clo) and metabolic rate (80 W/m<sup>2</sup>) and is only effective for people aged 20–60 (Höppe, 1999). UTCI sets walking speed at a constant 4 km per hour (1.11 m/s), internal heat production at 135 W/m<sup>2</sup>, and comes with an adaptive clothing model that adjusts to current conditions (Jendritzky et al., 2012). Their contribution to understanding and applying thermal stress and comfort in outdoor environments for children should not be overlooked in efforts to improve children's environmental health (Vanos, 2015). Thermal perception is influenced by numerous factors such as meteorological conditions, physiological factors, and thermal experiences (Elnabawi et al., 2016; Yin et al., 2012). Empirical thermal sensation models and thermal indices, which employ linear regression for prediction, are limited in their ability to fully reveal the complex causal relationships between thermal perception and its influencing factors.

To predict human thermal perception and comfort more accurately, machine learning has also been introduced into outdoor thermal comfort research. Mladenović et al. (2016) used support vector machines (SVM) to predict the thermal comfort index PET for visitors in open urban areas. Similarly, Kariminia et al. (2016) employed extreme learning machines (ELM) to predict the PET thermal comfort index of subjects in open areas in Iran. Liu et al. (2020) developed an SVM model to predict thermal comfort status in outdoor environments using local skin temperature and heat load as inputs. Eslamirad et al. (2020) proposed a novel method combining urban design strategies with supervised machine learning techniques, optimizing green walkways to improve outdoor thermal comfort while minimizing errors. Choropoulous et al. (2012) used artificial neural network (ANN) to predict the temperature-humidity index (THI) in a mountainous area of Greece. Based on the factors influencing PMV, Chan and Chau (2019) introduced microclimatic perception, environmental characteristic perception, and personal characteristics as additional predictive variables for thermal comfort, significantly improving the model's prediction performance. However, the established models require the input of an individual's psychological perception before predicting their thermal comfort. This method of predicting one perception using one or multiple perceptions impedes the practical application of the model. Therefore, the selection of input variables should be easily obtainable, as if the difficulty of obtaining input variables is comparable to or greater than that of output variables, the predictive significance is lost. Conducting questionnaire surveys to obtain subjective thermal perception evaluations from children, a distinct demographic from other age groups, often proves to be more complex (He et al., 2023). Thus, accurately predicting children's subjective thermal perception based on limited collected data appears particularly crucial. Li et al. (2024) monitored and collected physiological indicators, facial expressions, and subjective thermal evaluations of children in outdoor open spaces. They combined machine learning to construct a predictive model for children's outdoor thermal sensation based on non-intrusive data collection such as facial expressions, ear skin temperature, and heart rate. This achievement facilitates real-time monitoring of children's thermal comfort, ensuring their outdoor thermal health and safety. However, this model lacks connections with objective environmental characteristics.

ANN serves as one of the crucial algorithms in machine learning, renowned for their robust information processing capabilities, enabling the resolution of complex, mathematically uncertain, stochastic, and nonlinear problems (Basheer and Hajmeer, 2000; Graupe, 2013). They have been extensively employed in prediction, decision-making, classification, and control systems (Kalogirou, 2000). For example, they have been used in fraud detection (Omar et al., 2017), medical diagnosis (Amato et al., 2013), protein structure prediction (Hirst and Sternberg, 1992; Wardah et al., 2019), and agriculture (Khairunniza-Bejo et al., 2014; C. Yang et al., 2000). In architecture, they have optimized building energy use and thermal comfort. Given their adaptability and generalization

capabilities, they hold great potential for improving the accuracy of children's thermal perception predictions and enhancing outdoor thermal comfort (Deng and Chen, 2018; Mba et al., 2016; Shan et al., 2020).

In summary, this study aims to develop a comprehensive ANN model that considers traditional PMV factors, as well as additional personal characteristics and environmental variables, to predict outdoor thermal perception of children in Harbin, China. By comparing the predictive performance of the MLR, the UTCI, and the ANN models, the feasibility and superiority of ANN in predicting residents' outdoor thermal perception will be validated. Furthermore, this study will discuss the potential applications of the constructed model in park management, services, and the optimization of child-friendly park spaces, through feature sensitivity analysis and other methods. The research findings will provide valuable insights for urban planners and landscape designers regarding the development of child-friendly urban parks, contributing to the enhancement of children's well-being in outdoor thermal environments.

## 2. Methods

### 2.1. Data collection

The field survey in this study was conducted in Harbin, which is classified as a Dwa climate according to the Köppen-Geiger climate classification (Fig. 1) (Beck et al., 2023). Based on meteorological records from 1991 to 2021, we plotted the temperature and humidity conditions in Harbin over the years (Fig. 2), which shows that Harbin has very cold winters, hot summers, and a mild but dry transition season (China Meteorological Administration (CMA) (2025)). We collected data during the winter, summer, and transitional season on the following dates: January 12, 13, 14, 17, 18, and 19, 2022; July 6, 8, 9, 10, 11, and 12, 2022; April 8, and May 1, 2, 6, and 7, 2023. Fig. 3 illustrates the site conditions of the field survey and the seasonal Sky View Factors (SVF) at various measurement points. This study targeted children aged 4 to 17 years old and collected original data from four open spaces within an urban park in Harbin through meteorological data measurements and questionnaire surveys. These four representative spaces composed of plants represent open space, semi-enclosed space, enclosed space and covered space. And they are very popular with children. The database composed of these data would be utilized for predicting children's outdoor thermal perception. Considering the daylight duration in Harbin, the field survey times during winter were set from 8:30 to 15:30, while during the transitional and summer seasons, it extended from 8:30 to 16:30. A mobile microclimate station composed of instruments compliant with ISO 7726 was used to monitor the microclimate conditions at the survey locations, including  $T_a$ , RH, V, G, and black globe temperature ( $T_g$ ), were monitored using mobile microclimate stations. Fisheye photos of different spaces in different seasons were captured using an EOS 5D Mark III camera paired with an EF 8-15 mm f/4 L USM lens to calculate SVF. Our study employed non-invasive field observations and collected general demographic information such as children's gender, height, weight, age, activity type, and clothing with consent from the children or their guardians. Sensitive information such as names, addresses, and contact details were not collected (Appendix Fig. S1). Surveys were conducted through questionnaires combined with interviews, with the help of guardians when necessary. Detailed information on the survey methods and meteorological instruments can be found in reference (He et al., 2023).

Metabolic rate and clothing insulation are two important factors affecting thermal sensation besides meteorological parameters. Havenith (2007) proved that children's clothing insulation values are like those of adults in the same season, allowing the use of adult values for calculating children's insulation. This study evaluated children's clothing insulation values based on ISO 9920 (ISO

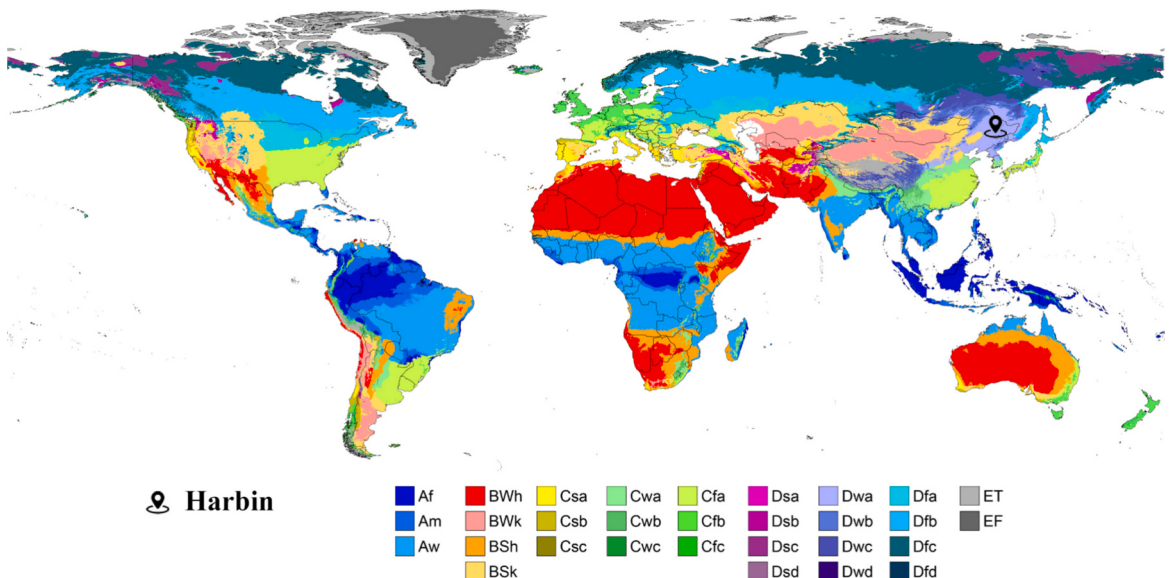


**Fig. 1.** The global maps of the Köppen-Geiger climate classification.

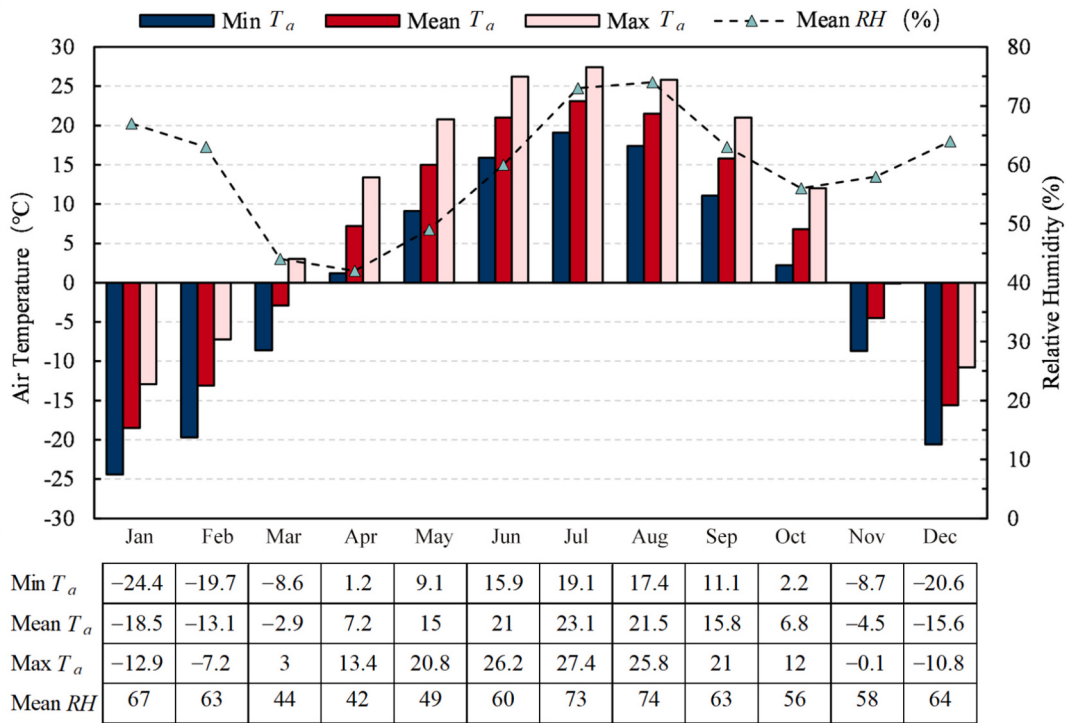


**Fig. 2.** Monthly mean/maximum/minimum air temperature ( $T_a$ ) and mean relative humidity (RH) in Harbin from 1991 to 2021.

International Standard 9920, 2007). Fig. 4 lists the clothing items and their insulation values. One Metabolic Equivalent of Task (MET) for adults represents the consumption of 3.5 mL of oxygen per kilogram of body weight per minute (i.e.,  $3.5 \text{ mL} \cdot \text{kg}^{-1} \cdot \text{min}^{-1}$ ), or the expenditure of 1 kcal of heat per kilogram of body weight per hour (i.e.,  $1 \text{ kcal} \cdot \text{kg}^{-1} \cdot \text{hr}^{-1}$ ). However, due to differences in metabolic characteristics, adult MET values may not be directly applicable to children. The basal metabolic rate per unit body weight for children and adolescents is higher than that for adults. Therefore, the energy expenditure per kilogram of body weight during physical activity is greater for children and adolescents than for adults. To accurately assess children's MET values, Butte et al. (2018) compiled a summary of children and adolescents' physical activity energy expenditure, presenting MET values for the same physical activity in four age groups: 6–9, 10–12, 13–15, and 16–18 years. In this study, the physical activity values for 4- and 5-year-old children were approximated using the MET values for 6–9 years (Table 1).

## 2.2. Development of ANN

### 2.2.1. Screening of predictor variables

Although the PMV algorithm had been shown to be inadequate in correctly predicting the ASHRAE mean vote, it was clear that the six factors influencing PMV do affect thermal sensation (von Grabe, 2016). Therefore, this study used four climatic variables ( $T_a$ ,  $V$ ,  $RH$ ,  $T_{mrt}$ ) and two personal variables ( $MET$ ,  $I_{cl}$ ) as initial input variables affecting thermal sensation. On this basis, the study employed Pearson correlation analysis to screen out objective variables significantly correlated with thermal sensation ( $P < 0.05$ ) as the final input variables. The additional input data included other environmental features ( $SVF$ ,  $T_g$ ,  $G$ ) and personal parameters ( $Height$ ,  $Weight$ ,  $BMI$ ,  $Age$ ,  $Sex$ ,  $Posture$ , etc.).

### 2.2.2. Data preprocessing

This study employed min-max normalization to scale the input and output variables to the range of  $[-1, 1]$ . After applying the min-max normalization process, each variable lay within the desired value range while maintaining the basic distribution of the corresponding variables.

$$x = 2 * \frac{x_0 - x_{\min}}{x_{\max} - x_{\min}} - 1 \quad (1)$$

In this context,  $x_0$  represents the original data, and  $x$  represents the normalized data. Since we used the normalized data for training, the predicted values were also based on the normalized data. Therefore, we denormalized the predicted values to obtain the actual predictions. The denormalization process was given by:

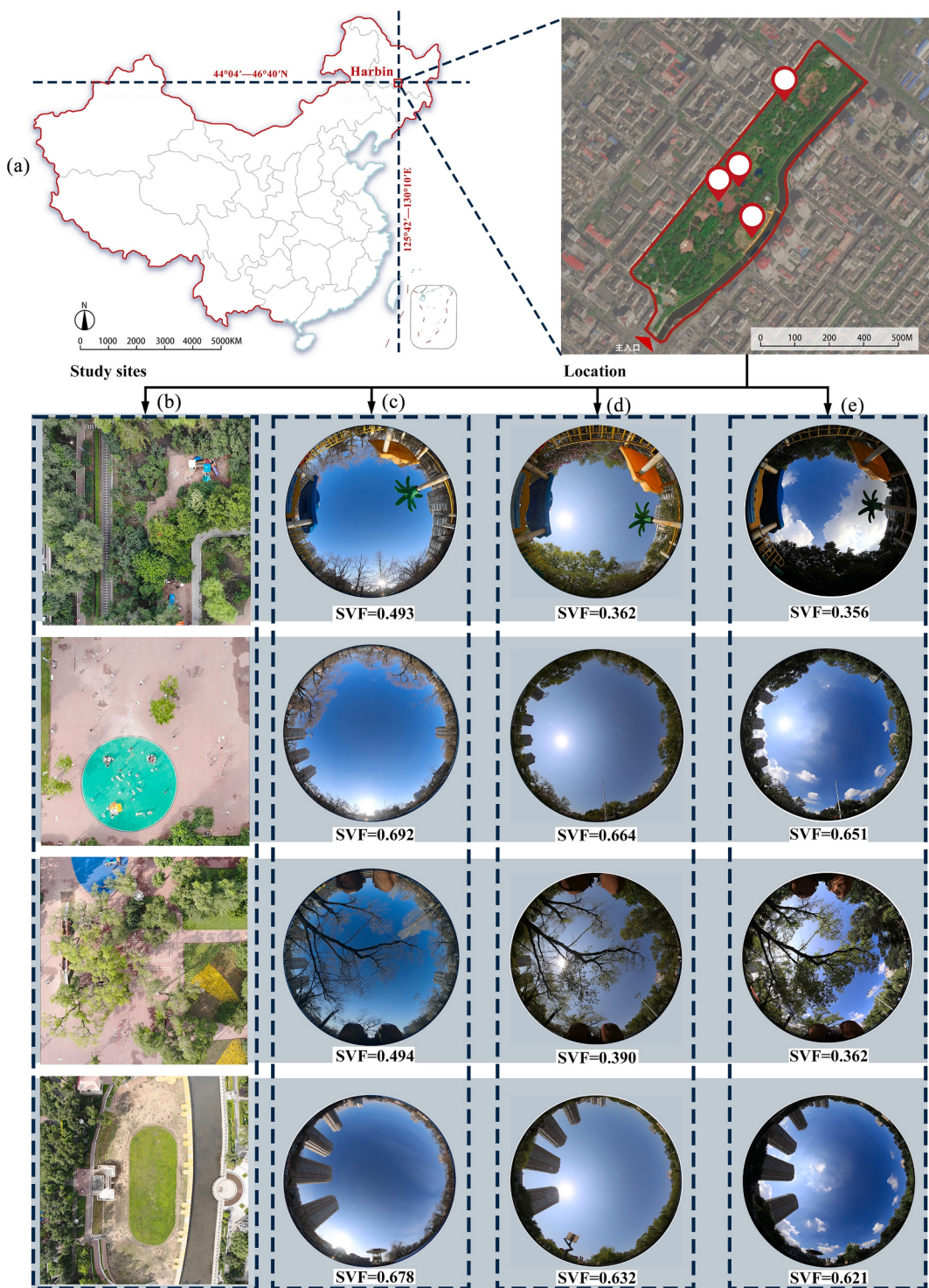


**Fig. 3.** Site location and measurement spaces: (a) site location; (b) photos of open spaces; (c) winter's fisheye photos; (d) spring's fisheye photos; (e) summer's fisheye photos.

<b>Clothes checklist</b>				
<b>Sundries:</b>	<input type="checkbox"/> Gloves 0.05 <input type="checkbox"/> Cap 0.01			
<b>Upper body:</b>	<input type="checkbox"/> Underwear T-shirt 0.08 <input type="checkbox"/> Underwear - Shirt, long sleeves 0.25 <input type="checkbox"/> Underwear-Shirt, long sleeves, thermal 0.2 <input type="checkbox"/> Short sleeve 0.15 <input type="checkbox"/> Vest 0.2 <input type="checkbox"/> Shirts ( <input type="checkbox"/> Light-weight 0.2 <input type="checkbox"/> Normal 0.25) <input type="checkbox"/> Down vest 0.3 <input type="checkbox"/> Down jacket 0.55 Sweater ( <input type="checkbox"/> Sleeveless 0.12 <input type="checkbox"/> Thin 0.20 <input type="checkbox"/> Thick 0.35) <input type="checkbox"/> Coat 0.6 Jacket ( <input type="checkbox"/> Thin 0.25 <input type="checkbox"/> Thick 0.35 <input type="checkbox"/> Fibre-pelt 0.4)			
<b>Lower body:</b>	<input type="checkbox"/> Shorts 0.06 <input type="checkbox"/> Underwear - Pants, long-legged, thermal 0.15 <input type="checkbox"/> Light skirts (summer) 0.15 <input type="checkbox"/> Light dress, short sleeves 0.2 <input type="checkbox"/> Flannel 0.28 <input type="checkbox"/> Underwear-Pants, long-legged 0.22 <input type="checkbox"/> Sweat pants 0.28 Trousers ( <input type="checkbox"/> Thin 0.15 <input type="checkbox"/> Thick 0.24)    Trousers ( <input type="checkbox"/> Light-weight 0.2 <input type="checkbox"/> Normal 0.25) <input type="checkbox"/> Trousers, fibre-pelt 0.4 <input type="checkbox"/> Winter dress, long sleeves 0.4			
<b>Feet:</b>	<input type="checkbox"/> Shoes ( <input type="checkbox"/> Thin-soled 0.02 <input type="checkbox"/> Thick-soled 0.04) <input type="checkbox"/> Boots 0.1 <input type="checkbox"/> Socks ( <input type="checkbox"/> Thin 0.02 <input type="checkbox"/> Thick & ankle 0.05 <input type="checkbox"/> Thick & long 0.1)			

Fig. 4. Simplified children's clothes checklist.

**Table 1**

Different types of children's activities and corresponding MET values.

MET Code	Activity Type	Specific Activity	MET			
			4-9	10-12	13-15	16-17
55,340X	Sitting	Sitting	1.4	1.3	1.3	1.2
70,200X	Standing	Standing	1.7	1.7	1.7	1.6
80,120X	Walking	Walking 1.0 mph / 1.6 km/h	2.5	2.6	2.7	2.8
80,180X	Walking	Walking 2.5 mph / 4.0 km/h	3.3	3.5	3.6	3.7
65,500X	Sports	Table tennis	4.2	4.2	4.2	4.2
25,140X	Cycling	Cycling (self-determined speed)	4.6	5.3	5.8	6.4
65,360X	Sports	Skateboarding (40 slides/min)	4.9	5.0	5.0	5.1
65,320X	Sports	Roller skating	5.2	5.2	5.3	5.4
60,120X	Running	Jogging: slow	5.5	5.9	6.3	6.7
10,160X	Playing	Free play: basketball, jump rope/climbing rope, hula hoop, climbing, ladder, frisbee	5.7	5.9	6.0	6.1
10,100X	Playing	Ball games: bouncing, soccer, dribbling, reaction ball	6.0	6.2	6.3	6.5
10,440X	Playing	Tag games	6.1	6.3	6.4	6.6
10,240X	Playing	Jumping house game	6.3	6.5	6.7	6.8
10,260X	Playing	Jump rope	6.9	7.1	7.2	7.4
60,100X	Running	Jogging: fast	7.2	7.9	8.5	8.8

$$x_0 = \frac{(x + 1)*(x_{max} - x_{min})}{2} + x_{min} \quad (2)$$

By using these formulas, we ensured that the predicted values reflect the actual scale of the data, preserving the interpretability and practical utility of the model's output.

### 2.2.3. The basic structure of ANN

Common types of neural networks include feedforward neural networks, recurrent neural networks, and graph neural networks. Feedforward neural networks can effectively reduce computational complexity and training difficulty while improving generalization ability. Therefore, this study adopted a feedforward neural network. A neural network consisted of an input layer, hidden layers, and an output layer. A sigmoid function was selected as the transfer function for the hidden layers, and a linear function was chosen for the output layer. The Levenberg-Marquardt algorithm was employed for network training. This algorithm was widely used in feedforward neural networks due to its speed and accuracy (Buratti et al., 2015; Deng and Chen, 2018).

In this study, after loading the data, the entire dataset was first divided into two parts. The first part, accounting for 80 %, was used to design the network, while the second part, comprising 20 %, served as an independent final test dataset (ITD), separate from the network design process. The first part of the data was further divided into a training dataset (TD, 60 %), a validation dataset (VD, 20 %), and a test dataset (ITD, 20 %).

%), and a test dataset (TestD, 20 %).

A neural network with a single hidden layer can approximate any function (Hecht-Nielsen, 1987; Hecht, 1989). However, more hidden layers enhance the neural network's ability to represent highly nonlinear assumptions. This study developed both single hidden layer and double hidden layer ANN models, using the same transfer functions, training methods, data partitioning, and normalization techniques. The primary difference between the two models lay in the number of hidden layers and the number of neurons in each hidden layer. The single hidden layer ANN model was developed using the Neural Network Toolbox in MATLAB.

Based on these, the study first constructed a single hidden layer ANN model to quickly assess the contribution of predictor variables to the model. Subsequently, a double hidden layer ANN model was developed to attempt to further enhance model performance. The number of neurons in the hidden layers can significantly impact the quality of the model. Although there was no definitive rule for determining the number of neurons in the hidden layers (Pentoš, 2016), their range be approximated using the following formula (Maier and Dandy, 2000):

$$2 \times \sqrt{N_i} + N_0 \leq N_h \leq 2 \times N_i + 1 \quad (3)$$

In this formula,  $N_0$  is the number of neurons in the output layer, which was 1 in this study (heat sensation votes),  $N_h$  represents the possible number of neurons in the hidden layer, and  $N_i$  is the number of neurons in the input layer.

There are several methods to enhance the generalization ability of a neural network, such as training multiple times to find the best generalization network, averaging the outputs of multiple neural networks, early stopping, and regularization. MATLAB's default method for improving generalization is called early stopping. Building on this, the study trained the network architecture 10 times, and the average of the outputs from these 10 networks was used as the final prediction result to avoid instability issues that might arise from relying on a single optimal network (Chan and Chau, 2019; de Oña and Garrido, 2014; Pentoš, 2016). This approach helped to ensure robustness and accuracy in the model's predictions, taking advantage of the ensemble of networks to mitigate the impact of any individual network's overfitting or underperformance.

### 2.3. Performance comparison with traditional models

#### 2.3.1. Predicting thermal perception by UTCI

Compared to other indices, the UTCI better describes the temporal variations in thermal conditions, more accurately representing specific climates, weather, and locations. It can be applied across all weather conditions, seasons, and spatial scales (Jendritzky et al., 2012).

The UTCI value was calculated using meteorological parameters such as  $T_a$ , RH, V, and  $T_{mrt}$ , among others, by inputting them into RayMan software.  $T_{mrt}$  was calculated using eqs. (4).

$$T_{mrt} = \left[ \left( T_g + 273 \right)^4 + \frac{1.10 \times 10^8 V^{0.6}}{\varepsilon D^{0.4}} \left( T_g - T_a \right) \right]^{\frac{1}{4}} - 273 \quad (4)$$

In Eqs. (2–4),  $D$  represents the diameter of the black globe ( $D = 0.05$  m), and  $\varepsilon$  represents the emissivity coefficient of the black globe ( $\varepsilon = 0.95$ ).

Essentially, this method used UTCI to equivalently measure the actual thermal environment people were exposed to and then employed a linear regression model to predict their subjective thermal perception. The traditional approach calculates the weighted average of thermal sensation vote (TSV) for each 1 °C UTCI interval to obtain mean TSV, which is then linearly regressed against UTCI (He et al., 2020; He et al., 2023). This method predicts the average TSV for a group of people, lacking consideration for individual differences. In this study, linear regression analysis was conducted using SPSS software on individual TSV datasets and their corresponding UTCI datasets. The regression equation is expressed as follows:

$$TSV = C + B * UTCI \quad (5)$$

#### 2.3.2. Prediction of thermal perception by MLR model

Based on climate data and personal data, thermal perception can be predicted. Salata et al. (2016) proposed the Mediterranean Outdoor Comfort Index (MOCI), which uses V, RH,  $T_{mrt}$ ,  $T_a$ , and clothing insulation values to predict the thermal sensation of Mediterranean people. Similarly, Ruiz and Correa (2015) developed the thermal comfort index for arid regions (IZA), which predicts population thermal perception using  $T_a$ , V, and RH. Lai et al. (2014b) defined thermal sensation using four meteorological parameters measured by weather stations:  $T_a$ , G, V, and RH. W. Yang et al. (2013) applied multiple linear regression to predict respondents' thermal sensation as a function of four variables:  $T_a$ , RH, V, and  $T_{mrt}$ . Cheng et al. (2012) developed a formula to predict thermal sensation using linear regression analysis with four independent variables:  $T_a$ , V, G intensity, and absolute humidity. Krüger and Rossi (2011) expressed thermal sensation as a function of  $T_a$ , V, and G. The commonality in these studies is the selection of easily obtainable factors that have been empirically verified to significantly impact thermal perception as predictor variables.

Numerous factors influence thermal perception, including  $T_a$ ,  $T_{mrt}$ , V, RH, metabolic rate, and clothing insulation. These are widely recognized as the primary variables affecting thermal sensation (Y. Yang et al., 2024). This study aimed to express the TSV as a function of these six factors. Using SPSS, a data analysis software, a multiple linear regression model was constructed to represent this relationship. The model can be expressed as follows:

$$TSV = b_0 + b_1 T_a + b_2 T_{mrt} + b_3 V + b_4 RH + b_5 MET + b_6 I_{cl} \quad (6)$$

### 2.3.3. Model performance evaluation

This study characterized the model's performance using methods such as Mean Squared Error (MSE), correlation coefficient (R), and coefficient of determination ( $R^2$ ). The optimal network was selected by comparing the MSE of the ANN on an independent test set. The MSE of the independent test set was considered the primary evaluation criterion, as better performance on the test set indicated superior generalization ability of the model. Furthermore, we employed the Mean Bias Error (MBE), Mean Absolute Error (MAE), Root Mean Square Error (RMSE), along with its systematic (RMSE<sub>S</sub>) and unsystematic (RMSE<sub>U</sub>) components to facilitate a comparative evaluation of the model performance (Qin et al., 2021).

The predictive performance of the constructed ANN model was examined by comparing it with multiple linear regression models and the UTCI-TSV prediction model. The R was used to assess the degree of correlation between the ANN model's predictions and the actual values (TSV values collected during the survey). The  $R^2$  represented the proportion of variance explained by the model. The formulas for these calculations are as follows:

$$MSE = \frac{1}{n} \sum_{i=1}^n (\hat{y}_i - x_i)^2 \quad (7)$$

$$R = \frac{\sum_{i=1}^n (x_i - \bar{x})(y_i - \bar{y})}{\sqrt{\sum_{i=1}^n (x_i - \bar{x})^2} \sqrt{\sum_{i=1}^n (y_i - \bar{y})^2}} \quad (8)$$

$$R^2 = 1 - \frac{\sum_{i=1}^n (x_i - y_i)^2}{\sum_{i=1}^n (y_i - \bar{y})^2} \quad (9)$$

where  $x_i$  is the actual value,  $y_i$  is the predicted value,  $n$  is the number of observations,  $\bar{x}$  and  $\bar{y}$  are the mean values of the actual and predicted values, respectively.

### 2.4. Determine the importance order of variables based on sensitivity analysis

Sensitivity analysis is an effective method for determining the importance of variables in an ANN. The Sensitivity Coefficient (SC) is the ratio of the change in the output to the change in the input when all other parameters are held constant. There are various methods for conducting sensitivity analysis, with the simplest being the method of altering one parameter at a time while keeping all other parameters unchanged (Hamby, 1994). The ratio of the output change to the input change before and after the parameter alteration can be expressed as follows:

$$\Delta Y = Y(Xi + \Delta X) - Y(Xi) \quad (10)$$

**Table 2**  
Descriptive Statistics of the Data.

Parameter types		Content	Minimum	Maximum	Mean	Standard Deviation
PMV parameters	1	$T_a$ (°C)	-22.4	32.7	8.1	19.6
	2	RH (%)	14.3	82.0	48.0	13.3
	3	$V$ (m/s)	0.0	2.0	0.9	0.4
	4	$T_{mrt}$ (°C)	-22.3	74.7	28.9	22.1
	5	$I_{cl}$ (clo)	0.17	2.82	1.05	0.72
	6	MET	1.2	7.4	4.1	1.9
Environmental parameters	7	$G$ (W/m <sup>2</sup> )	24.0	1047.9	311.7	247.7
	8	$T_g$ (°C)	-21.6	43.9	13.2	19.8
	9	SVF	0.356	0.692	0.528	0.136
Personal parameters	10	Posture*	0	1	0.92	0.28
	11	High (cm)	90.0	188.0	143.5	17.6
	12	Weight (kg)	13.0	90.0	37.5	12.5
	13	BMI	10.1	33.3	17.8	3.5
	14	Age	4.0	17.0	10.1	2.9
Dependent variable	15	Sex**	0	1	0.6	0.5
	16	TSV	-4	4	0.54	1.987

\* Standing: 1, Sitting: 0.

\*\* Male: 1, Female: 0.

$$SC = \frac{\Delta Y}{\Delta X} \quad (11)$$

The perturbation value  $\Delta X$  stands for a minor change in the parameter. In this study, we increased each parameter by 1 %, which, after normalization, equated to an increase of 0.01. By altering the input parameters by this amount while keeping all other parameters constant, we recorded the changes in the output. Then, we calculated the SC for each parameter using the method described. This approach was systematically applied to all parameters.

### 3. Results

#### 3.1. Basic data description

A total of 1616 valid questionnaires were collected during the field survey. Table 2 presents the statistical data of 15 potential factors influencing the TSV. These include six factors confirmed by previous studies to influence thermal perception, along with three environmental characteristics:  $G$ ,  $T_g$ , and  $SVF$ . Additionally, six personal characteristics were recorded: *Height*, *Weight*, *Sex*, *Age*, *Body mass index (BMI)*, and *Posture*. Interestingly, the minimum recorded  $T_a$  was  $-22.4$  °C, while the maximum  $T_a$  reached  $32.7$  °C, indicating a significant temperature variation between the cold and hot seasons in Harbin. Correspondingly, children's clothing insulation values ranged widely from 0.17 clo to 2.82 clo. The ages of the children ranged from 4 to 17 years, with an average age of 10.1 years. We conducted a Kruskal-Wallis H test to examine differences in thermal sensation among children of different age groups (Appendix Table S1). The results indicate that at the 0.01 significance level, children aged 16–17 exhibited significantly different thermal sensations compared to the 4–9 and 10–12 age groups. This difference may be attributed to older children being physiologically closer to adults, whose thermal perception has been shown to differ significantly from that of younger children (Mors et al., 2011). Male children accounted for 60 % of the total participants. Most of the children were standing (92 %), with a few sitting (8 %). The activity intensity of children in the park's open spaces averaged moderate-light intensity at 4.1 MET.

Fig. 5 illustrates the percentage distribution of TSVs across different seasons. In winter, children's thermal sensations were primarily reported as 'cold' (16.1 %), 'cool' (22.4 %), 'slightly cool' (26.9 %), and 'neutral' (24.4 %). In spring, the most frequent TSV was 'neutral' (36.2 %). In summer, the highest percentages were 'hot' (32.6 %), followed by 'very hot' (19.5 %) and 'neutral' (19.5 %). Overall, across the three seasons and a total of 1616 observations, the highest overall TSV percentage was 'neutral' (27 %), followed by 'hot' (15.9 %) and 'slightly cool' (14.3 %). The mean TSV across all observations was 0.54, indicating a slight tendency towards a warmer sensation than 'neutral', with a standard deviation of 1.987.

#### 3.2. Development of traditional models

##### 3.2.1. The UTCI model

To evaluate the predictive performance of UTCI on TSV, a simple linear regression analysis was conducted between TSV and UTCI (Table 3). The results indicated that UTCI can significantly predict variations in children's TSV, with  $\beta = 0.708$ ,  $t = 40.247$ , and  $P < 0.001$ . UTCI explained 50.1 % of the variance in TSV. The linear regression equation between TSV and UTCI was expressed as follows:

$$TSV = -0.478 + 0.073UTCI \quad (12)$$

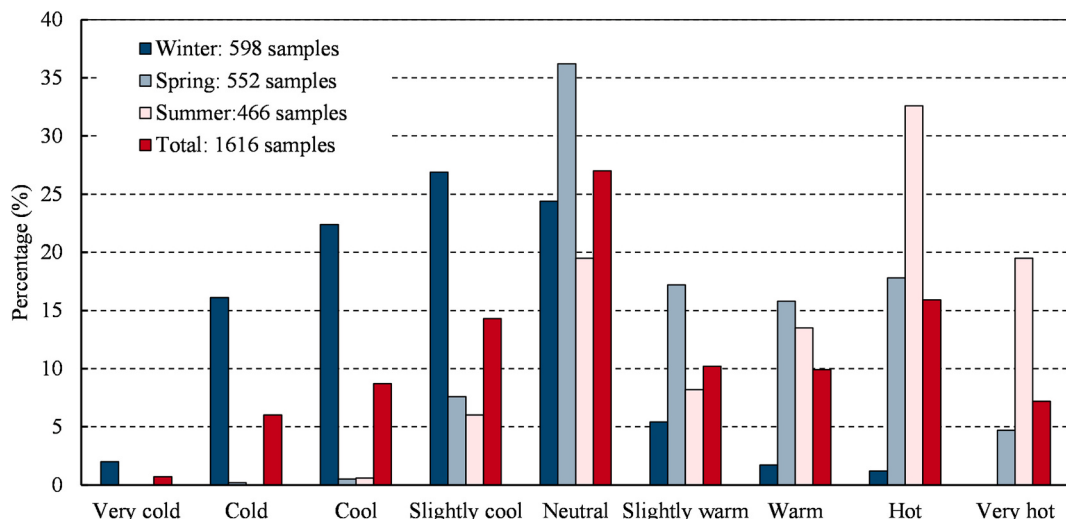


Fig. 5. Percentages of thermal sensation votes in different seasons.

**Table 3**

Linear regression analysis of children's thermal perception and UTCI.

	B	Constant	$\beta$	R <sup>2</sup>	t	F	P
Total	0.073	-0.478	0.708	0.501	40.247	1619.803	<0.001

**Table 4**

Collinearity test between predictor variables.

	VIF-total	VIF-total (after delete $I_{cl}$ )
T <sub>a</sub>	17.031	4.495
RH	1.178	1.166
V	1.956	1.954
T <sub>mrt</sub>	4.783	4.780
I <sub>cl</sub>	13.718	—
MET	1.019	1.019

### 3.2.2. The MLR model

Multicollinearity occurs when two or more independent variables are highly correlated, which can affect both the explanation of the dependent variable's variance and the overall fit of the multiple linear regression model. Therefore, this study first examined the collinearity among the six PMV factors (Table 4). There was significant collinearity between  $T_a$  and  $I_{cl}$  (Variance Inflation Factor, VIF > 10). Considering that people tend to adjust their clothing based on temperature changes,  $I_{cl}$  was excluded from the multiple linear regression predictive model. Thus, the variables  $T_a$ , RH, V,  $T_{mrt}$ , and MET were used as independent variables in the model.

Table 5 indicates that the regression model is statistically significant ( $P < 0.001$ ). The five variables explain 52.7 % of the variance in TSV. The significance tests for the variables show that  $T_a$ ,  $T_{mrt}$ , and MET can significantly predict children's TSV. The multiple linear regression model for predicting children's thermal sensation in Harbin is represented by Eq. (13).

$$\text{TSV} = 0.048T_a - 0.003RH - 0.219V + 0.025T_{mrt} + 0.161\text{MET} - 0.892 \quad (13)$$

### 3.3. Development of ANN models

#### 3.3.1. Feature selection and basic structure

This study used the four climatic variables and two personal variables proposed by Fanger in the PMV algorithm as the initial input features for the ANN model (Fanger, 1970). Based on this, a Pearson correlation analysis was conducted on other features recorded during the field survey (Fig. 6). Features significant at the 0.05 level were included in the ANN model. Ultimately, three personal parameters—Posture, BMI, and Sex—were excluded due to their insignificant correlation with TSV, while G,  $T_g$ , SVF, Height, Weight, and Age were included as input variables for the ANN model.

#### 3.3.2. Development of ANN model

We designed and tested two different neural network architectures (Appendix Table S2, Fig. S2 and S3), the ANN model with two hidden layers performs better. Table 6 shows its specific performance. The R on the training set, validation set, and test set were close to each other. It indicated that the model had good generalization ability. The minimum MSE was 0.1107, the maximum was 0.1148, and the average was 0.1134, which outperforms the one-hidden-layer ANN model (Appendix Table S3).

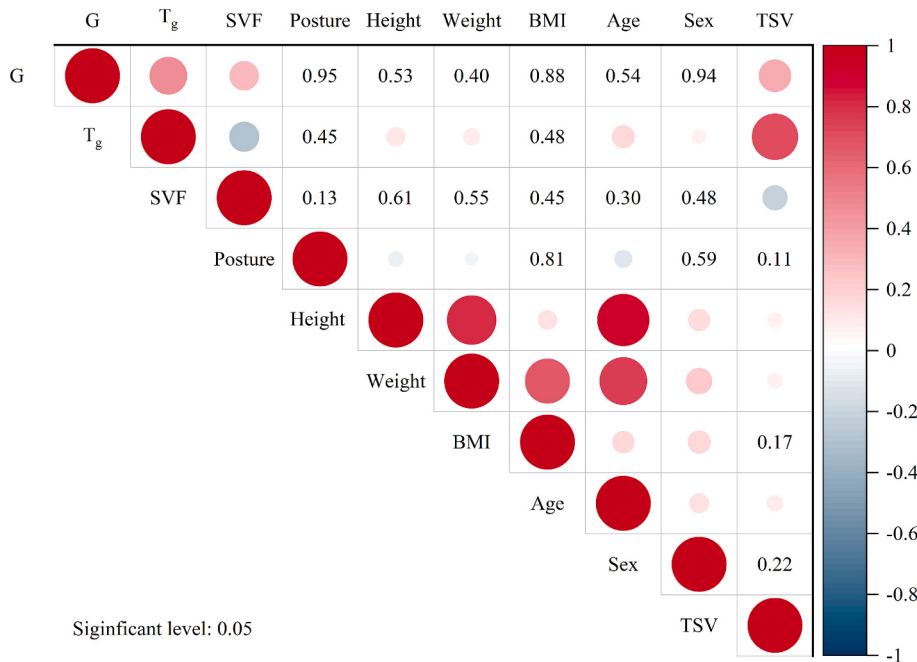
### 3.4. Comparison of traditional models and ANN models

Table 7 presents the results of linear regression analysis for the predicted values of four models against the actual values. The R of the two-hidden-layer ANN was slightly greater than that of the single hidden layer ( $0.755 > 0.748$ ), surpassing the other two traditional models. The MBE indicates that the systematic bias of all four models is relatively small. The RMSE<sub>S</sub> of all models is less than the

**Table 5**

Multiple linear regression of TSV and six PMV factors.

	B	$\beta$	t	P
Ta	0.048	0.468	12.853	0.000
RH	-0.003	-0.020	-1.099	0.272
V	-0.219	-0.044	-1.832	0.067
Tmrt	0.025	0.282	7.523	0.000
MET	0.161	0.151	8.688	0.000
Constant	-0.892		-4.673	0.000
Adjusted R2	0.524			
F	F = 356.026, p = 0.000			



**Fig. 6.** Pearson correlation analysis of ANN model potential input variables and TSV.

**Table 6**

The 10 optimal two-hidden-layer ANN models with the best performance on the ITS.

No	Structure	R			TestS	MSE <sub>ITS</sub>
		TS	VS	TestS		
1	12-20-9-1	0.7585	0.7106	0.6894		0.1107
2	12-23-14-1	0.7482	0.7092	0.7262		0.1114
3	12-19-8-1	0.7549	0.7036	0.7140		0.1120
4	12-12-9-1	0.7523	0.7143	0.6517		0.1136
5	12-13-19-1	0.7805	0.6745	0.6203		0.1139
6	12-19-12-1	0.7566	0.7258	0.6849		0.1143
7	12-8-14-1	0.7586	0.6972	0.6991		0.1145
8	12-22-9-1	0.7572	0.6933	0.6915		0.1145
9	12-16-20-1	0.7620	0.6919	0.7327		0.1147
10	12-16-10-1	0.7496	0.7181	0.7096		0.1148
Mean		0.7578	0.7039	0.6919		0.1134

**Table 7**

Linear regression analysis and predictive performance of (1) UTCI model, (2) MLR model, (3) one-hidden-layer ANN model, and (4) two-hidden-layer ANN model.

Model	B	R <sup>2</sup>	R	MSE	RMSE	RMSE <sub>S</sub>	RMSE <sub>U</sub>	MBE	MAE
(1)	0.5035	0.5009	0.708	1.968	1.403	0.006	1.403	-0.006	1.176
(2)	0.5494	0.5268	0.726	1.884	1.373	0.118	1.367	0.118	1.137
(3)	0.5436	0.5596	0.748	1.740	1.319	0.032	1.319	-0.032	1.085
(4)	0.5528	0.5701	0.755	1.697	1.303	0.007	1.303	-0.007	1.069

RMSE<sub>U</sub>, which indicates that the error is mainly due to random noise in the data rather than systematic. Among the four models, the two-hidden-layer ANN model had the smallest MSE (1.697), followed by the one-hidden-layer ANN model (1.740), the MLR model (1.884), and the UTCI model (1.968). Moreover, the MSE values also revealed that the two-hidden-layer ANN model performed best. Both RMSE and MAE exhibited trends like those of MSE.

It is worth noting that we tested the performance of the two-hidden-layer ANN model across different age groups and found that it performed better (with a higher R<sup>2</sup>) in predicting thermal perception for younger children compared to the 16–17 age group (Appendix Table S4). This is similar to actual thermal sensation, which may also be attributed to the fact that children's thermal perception differs significantly from that of adults (Zheng et al., 2024). Compared to younger children, children aged 16–17 have

physiological metabolism and other characteristics that are more like those of adults. To make a more specific comparison of the performance of the four models, we calculated the prediction accuracy by counting the number of votes where the predicted TSV matched the actual TSV, then dividing the result by the total number of votes and multiplying by 100 % (Su et al., 2024). The prediction accuracy of the UTCI model, MLR model, one-hidden-layer ANN model, and two-hidden-layer ANN model are 22.3 %, 23.3 %, 24.9 %, and 25.6 %, respectively (Appendix Table S5). This further demonstrates that the two-hidden-layer ANN model is the best among the four models.

Fig. 7 illustrates the linear regression relationships between the predicted and actual values for the four models. The  $R^2$  for the two-hidden-layer ANN model (0.5701) was greater than that of the UTCI model (0.5009), MLR model (0.5268), and one-hidden-layer ANN

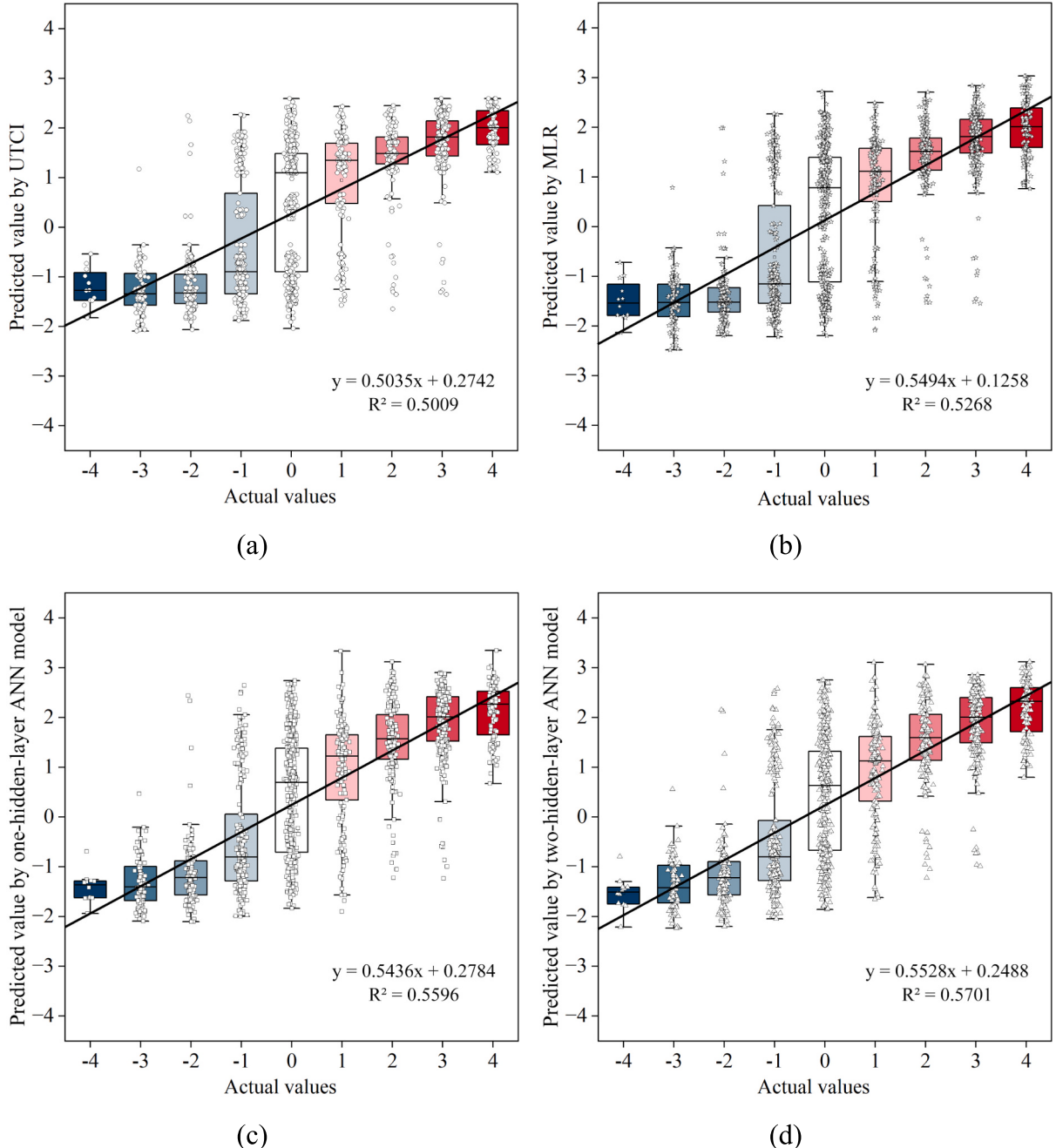


**Fig. 7.** The values predicted by (a) UTCI model, (b) MLR model, (c) one-hidden-layer ANN model, and (d) two-hidden-layer ANN model against the actual values.

model (0.5596). It is noteworthy that the two-hidden-layer ANN model improved the  $R^2$  values by 0.0692 and 0.0433 over the UTCI model and MLR model, respectively, but did not significantly enhance the predictive accuracy compared to the one-hidden-layer ANN model, with only a slight increase in the  $R^2$  value by 0.0105. This may be attributed to the fact that factors influencing thermal perception include, but are not limited to, meteorological conditions (Villadiego and Velay-Dabat, 2014), Environmental characteristics (Chan and Chau, 2019), physiological factors (Y. Zhang et al., 2020), clothing insulation (Y. Yang et al., 2024), psychological factors (Elnabawi et al., 2016), socioeconomic background (Shooshtarian, 2015), thermal experience (Krüger et al., 2017), and cultural differences (He et al., 2020). Some studies have even demonstrated that thermal perception is associated with aesthetic and auditory perceptions (Lau and Choi, 2021). In summary, thermal perception is a subjective variable influenced by multiple factors, and there are large differences between different individuals. In addition, the variables that can be quantified in our study are very limited. The predictive capability of the existing input features has likely reached its upper bound.

### 3.5. Predictor importance order

The multiple linear regression analysis provided insights into the contribution of each predictor variable to thermal sensation prediction. In section 3.2.2, the multiple linear regression analysis showed that among the six PMV factors,  $T_a$ ,  $T_{mrt}$ , and MET were the most significant predictors of TSV. In contrast, RH and V did not significantly contribute to TSV prediction. The ANN prediction model not only exhibited better performance compared to traditional models but also identified the contributions of different input variables to predicting children's thermal sensation through sensitivity analysis.

Fig. 8 illustrates the sensitivity coefficients of all input variables in the two-hidden-layer ANN model. A positive value indicates that changes in the input parameters are consistent with changes in thermal sensation, while a negative value indicates the opposite direction. The higher the absolute value, the more sensitive the thermal sensation is to changes in the input variables. The results show that  $T_{mrt}$ ,  $T_a$ ,  $T_g$ , MET, Height, Weight,  $I_{cl}$ , and G had positive contributions to TSV changes, while Age, V, and RH had negative contributions.  $T_{mrt}$  had the highest contribution to predicting TSV (SC = 0.259), followed by  $T_a$  (0.200),  $T_g$  (0.161), MET (0.110), Height (0.081), Age (-0.077), Weight (0.054), V (-0.044), RH (-0.022),  $I_{cl}$  (0.019), and G (0.016). The prominent contributions of  $T_{mrt}$ ,  $T_a$ , and MET to TSV prediction, as well as the small sensitivity coefficients of RH and V, were consistent with the results of the multiple linear regression analysis. The results also indicated that PMV factors significantly contributed to predicting children's TSV, while personal parameters such as Age, Height, and Weight also played important roles in predicting children's TSV.

It is worth noting that the sensitivity coefficient (0.0001) of TSV to SVF variations in this study was very small. However, the impact of SVF on TSV has been confirmed by many studies (Chiang et al., 2023; Lin et al., 2010). One possible reason for this discrepancy is that the differences in SVF between winter and spring in Harbin were relatively minor and they had not reached the minimum SVF threshold necessary to cause TSV changes. More importantly, Lam et al. (2023) pointed out in their study that SVF is an important predictor for the "warm group" (feeling warm and wanting to cool down), rather than the "neutral group" (feeling neutral and remaining unchanged). However, in this study, the highest proportion of TSV was 'Neutral' (27%). These factors might hindered the role of SVF in predicting TSV.

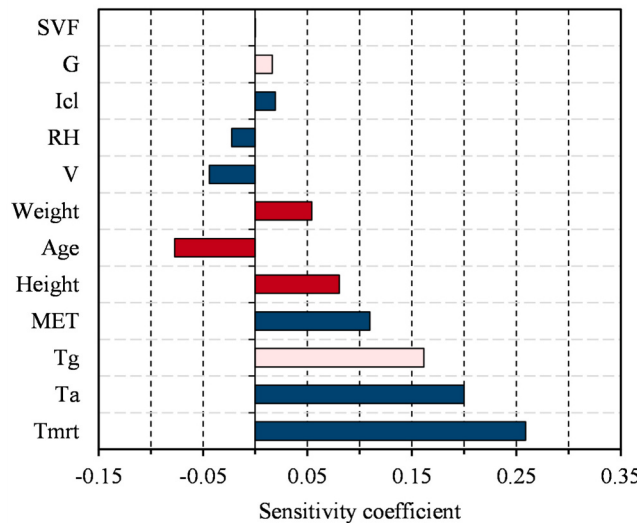


Fig. 8. Order of importance of the input variables.

**Table 8**  
Correspondence between thermal sensation and heat stress.

	Thermal sensation category	Thermal stress category
4	Very hot	Extreme heat stress
3	Hot	Strong heat stress
2	Warm	Moderate heat stress
1	Slightly warm	Slightly heat stress
0	Neutral	No thermal stress
-1	Slightly cool	Slightly cold stress
-2	Cool	Moderate cold stress
-3	Cold	Strong cold stress
-4	Very cold	Extreme cold stress

## 4. Discussion

### 4.1. Application prospects of ANN model

#### 4.1.1. Designer's auxiliary tools

Thermal sensation corresponds to thermal stress (Table 8) (Chen et al., 2020; Matzarakis and Mayer, 1996). The sensitivity coefficients not only elucidated the contribution of each parameter to the prediction of TSV but also provided valuable insights for designing child-friendly parks aimed at mitigating thermal stress. In selecting predictive variables, this study employed objective and quantifiable parameters as potential inputs for the ANN model, deliberately excluding children's subjective perceptions of wind, humidity, and temperature. These subjective factors have been proven to significantly enhance the predictive performance of ANN models (Chan and Chau, 2019), but their inclusion was avoided to maintain the practicality of the model. Incorporating subjective elements necessitates prior acquisition of these perceptions during the prediction process, which would render the model redundant, as direct collection of thermal sensation would be more straightforward.

The sensitivity coefficients of these objective variables revealed their significant impact on TSV. The ANN prediction model can thus serve as a valuable tool for assessing and refining design schemes. For example, if children exhibit lower TSV in a particular space during winter, indicating increased cold stress, designers can address this by incorporating facilities that encourage higher-intensity activities for children, since the sensitivity analysis shows that changes in MET correlate with changes in TSV. Furthermore, simulating microclimates for different design schemes is feasible with current technology. By using meteorological simulation software, the microclimates of various sites can be simulated. The resulting meteorological parameters, combined with individual parameters of the target demographic, can be input into the ANN thermal sensation prediction model to evaluate the effectiveness of the design schemes in mitigating thermal stress for the target population. This approach allows urban planners and landscape designers to strategically adjust and optimize design schemes based on the evaluation results to better meet the thermal needs of child users (Fig. 9).

#### 4.1.2. Smarter weather forecast

Traditional weather forecasts have supplied numerous conveniences for people's daily lives and activities. In indoor settings, individuals can more readily anticipate adjustments to clothing and physical activities in response to temperature forecasts, as indoor thermal conditions typically exhibit greater stability compared to outdoor environments. However, when individuals receive outdoor temperature forecasts from weather reports, they may find it challenging to fully comprehend the implications for their thermal comfort and necessary adjustments. Using thermal indices, such as UTCI and PET, as forecast values allow laypeople to assess the real outdoor thermal environment based on personal experience. Because these indices incorporate all climate parameters relevant to heat, including  $T_a$ , RH, V, and radiant temperature (Höppe, 1999). Nevertheless, as discussed in the introduction, these indices have certain limitations.

Therefore, even if UTCI or PET is reported in weather forecasts, individuals still need to autonomously adjust their thermal expectations based on subjective characteristics related to clothing and activities. The ANN-based thermal perception prediction developed in this study incorporates environmental characteristics, including meteorological parameters, as well as individual parameters such as behavioral activities. This enables potential users of outdoor spaces to forecast their thermal perception based on planned activities and clothing choices under specific environmental conditions. This implies that the model can also supply recommendations for activities and clothing that make thermal perception more neutral or suggest choosing appropriate spaces as destination. In short, the ANN prediction model also holds enormous potential in providing intelligent services related to urban park open spaces (Fig. 10).

### 4.2. Limitations and future research

Despite the promising results, this study still has some limitations that are worth considering in future research. Firstly, this study conducted field surveys on representative days selected from different seasons. It is well known that for training artificial neural networks, larger and more diverse datasets are advantageous for establishing high-performance models. Future research should involve monitoring and recording physical environmental data monthly, or even weekly, and conducting corresponding questionnaire surveys to obtain more comprehensive and extensive foundational data for developing ANN. Secondly, the richness of model input

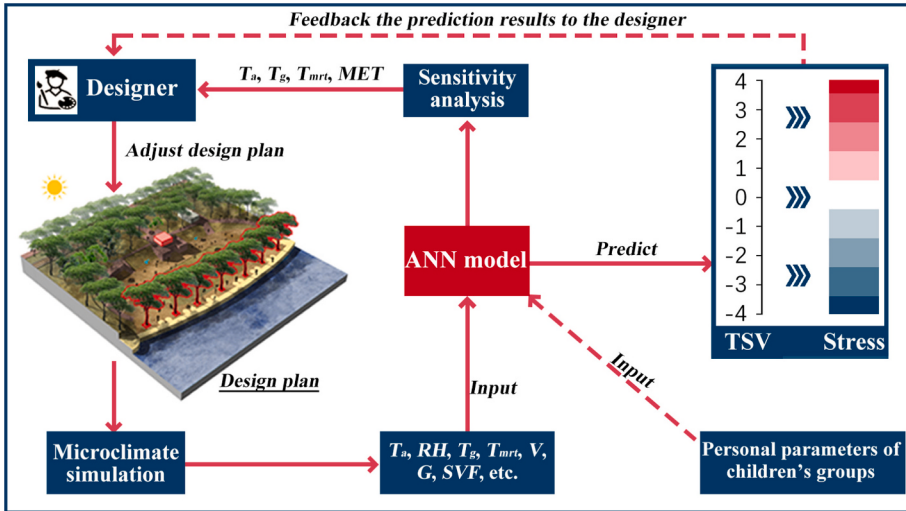


**Fig. 9.** Schematic diagram of ANN model assisting designers in formulating design plans.

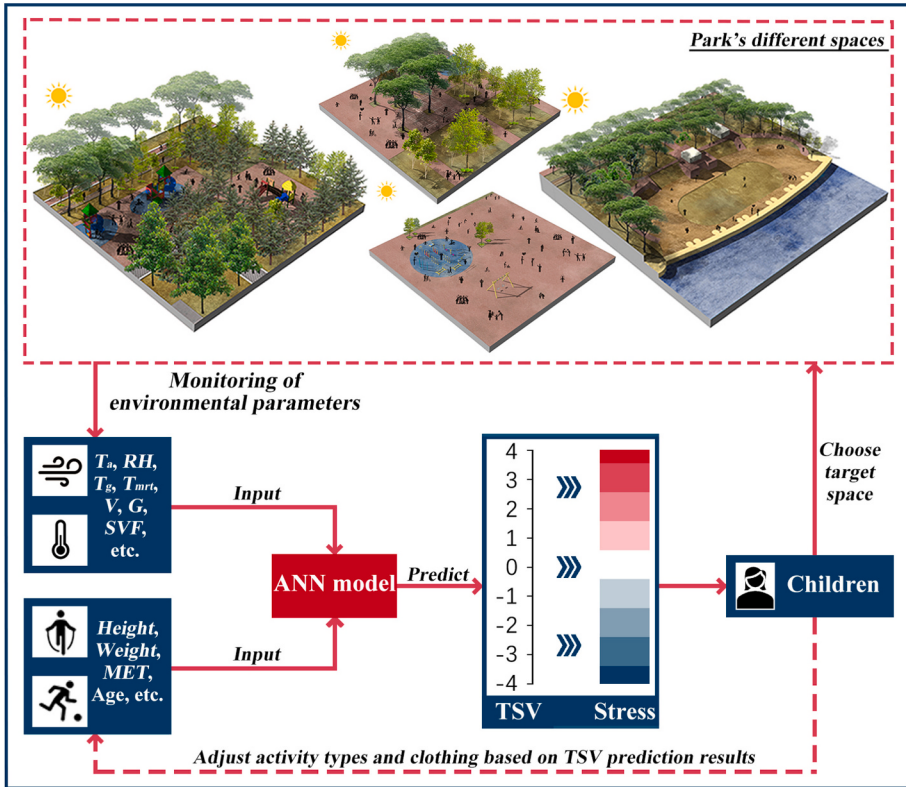


**Fig. 10.** Schematic diagram of ANN model as a park intelligent service assistant.

features is also crucial. This study selected easily measurable and quantifiable features such as meteorological parameters, environmental parameters, and personal parameters as predictive variables. These predictive variables could explain up to 57.01 % of the variation in children's TSV. This also confirms that the factors affecting human thermal perception are complex and diverse. For example, studies have shown that acoustic environment, light intensity (Geng et al., 2021), and emotional regulation (T. Zhang et al., 2021) also influence thermal sensation. Therefore, future research should consider more comprehensive selection of quantified environmental features to enhance the predictive performance of ANN models. Finally, this study briefly discussed the potential applications of ANN prediction models. However, the feasibility of these insights was not verified. Future research should focus on the

integration of artificial intelligence (AI) with urban park design and services, exploring how ANN models and other AI tools can be practically applied to improve park layouts and services to better mitigate heat stress and enhance the overall well-being of park users.

## 5. Conclusion

This study developed an ANN model to predict thermal sensation of children in urban open spaces, using 12 variables as predictive variables, including traditional PMV factors, additional environmental parameters, and personal parameters. The main conclusions are as follows. Firstly, for the prediction of TSV, the average R values of the top 10 networks in the training dataset, validation dataset, and testing dataset for the two-hidden-layer ANN were 0.7578, 0.7039, and 0.6919, respectively. Their proximity indicated that the model has good generalization ability. Secondly, compared to traditional models, the predictive performance of the ANN model was superior. The two-hidden-layer ANN model had the smallest MSE value (1.697), followed by the one-hidden-layer ANN model (1.740), the MLR model (1.884), and the UTCI model with the largest MSE value (1.968). The  $R^2$  values of these four models were 0.5701, 0.5596, 0.5268, and 0.5009, respectively. Furthermore, compared to the one-hidden-layer ANN model ( $R^2 = 0.5596$ ,  $B = 0.5517$ ,  $MSE = 1.740$ ), the improvement in predictive performance of the two-hidden-layer ANN model was limited ( $R^2 = 0.5701$ ,  $B = 0.5583$ ,  $MSE = 1.697$ ). Although the ANN model improves predictive performance, its effectiveness remains limited. This may be attributed to the fact that the contribution of the quantified predictor variables in this study has reached a plateau. Achieving better performance would require the model to learn from a larger and more diverse dataset. Lastly, sensitivity analysis revealed the sensitivity order of TSV to different features, from greatest to smallest:  $T_{mrt}$  (0.259),  $T_a$  (0.200),  $T_g$  (0.161),  $MET$  (0.110),  $Height$  (0.081),  $Age$  (-0.077),  $Weight$  (0.054),  $V$  (-0.044),  $RH$  (-0.022),  $I_{cl}$  (0.019), and  $G$  (0.016). While SVF (0.0001) did not significantly contribute to predicting TSV.

In summary, ANN models not only outperform traditional models in terms of predictive performance, but also address the limitations of thermal indices like UTCI and PET. These indices, due to their generalization and lack of testing on children, can lead to inaccurate estimates of physiological stress. Blindly relying on these indices could have serious consequences, such as misidentifying health issues in children (Höppe, 1999). ANN models incorporate personalized parameters, including height, weight, age, metabolic rate of physical activity, and clothing insulation values, as well as environmental characteristics like meteorological parameters and SVF, demonstrating a broader adaptive capacity that is well-suited for children. Our findings will offer valuable insights into predicting outdoor thermal sensation and assessing thermal comfort.

## Funding

This work was supported by the China Scholarship Council (CSC) [grant number 202306120268], and the National Natural Science Foundation of China [grant numbers 51908170].

## Author statement

This manuscript has not been published or presented elsewhere in part or in entirety and is not under consideration by another journal. All study participants provided informed consent. We also have read and understood your journal's policies, and we believe that neither the manuscript nor the study violates any of these.

## CRediT authorship contribution statement

**Xiaoyun He:** Writing – review & editing, Writing – original draft, Visualization, Validation, Software, Methodology, Investigation, Formal analysis, Data curation, Conceptualization. **Kerry A. Nice:** Writing – review & editing, Supervision. **Yuexing Tang:** Resources, Project administration, Investigation, Funding acquisition. **Long Shao:** Supervision, Conceptualization.

## Declaration of competing interest

The authors declare that they have no known competing financial interests or personal relationships that could have appeared to influence the work reported in this paper.

## Acknowledgments

None.

## Appendix A. Supplementary data

Supplementary data to this article can be found online at <https://doi.org/10.1016/j.uclim.2025.102378>.

## Data availability

Data will be made available on request.

## References

- Amato, F., López, A., Peña-Méndez, E.M., Vainhara, P., Hampl, A., Havel, J., 2013. Artificial neural networks in medical diagnosis. *J. Appl. Biomed.* 11 (2), 47–58. <https://doi.org/10.2478/v10136-012-0031-x>.
- Basheer, I.A., Hajmeer, M., 2000. Artificial neural networks: fundamentals, computing, design, and application. *J. Microbiol. Methods* 43 (1), 3–31. [https://doi.org/10.1016/S0167-7012\(00\)00201-3](https://doi.org/10.1016/S0167-7012(00)00201-3).
- Beck, H.E., McVicar, T.R., Vergopolan, N., Berg, A., Lutsko, N.J., Dufour, A., Zeng, Z., Jiang, X., van Dijk, A.I.J.M., Miralles, D.G., 2023. High-resolution (1 km) Köppen-Geiger maps for 1901–2099 based on constrained CMIP6 projections. *Sci. Data* 10 (1), 724. <https://doi.org/10.1038/s41597-023-02549-6>.
- Buratti, C., Vergoni, M., Palladino, D., 2015. Thermal comfort evaluation within non-residential environments: development of artificial neural network by using the adaptive approach data. *Energy Procedia* 78, 2875–2880. <https://doi.org/10.1016/j.egypro.2015.11.656>.
- Butte, N.F., Watson, K.B., Ridley, K., Zakeri, I.F., McMurray, R.G., Pfeiffer, K.A., Crouter, S.E., Herrmann, S.D., Bassett, D.R., Long, A., 2018. A youth compendium of physical activities: activity codes and metabolic intensities. *Med. Sci. Sport.* 50 (2), 246. <https://doi.org/10.1249/MSS.0000000000001430>.
- Chai, Q., Wang, H., Zhai, Y., Yang, L., 2020. Using machine learning algorithms to predict occupants' thermal comfort in naturally ventilated residential buildings. *Energ. Buildin.* 217, 109937. <https://doi.org/10.1016/j.enbuild.2020.109937>.
- Chan, S.Y., Chau, C.K., 2019. Development of artificial neural network models for predicting thermal comfort evaluation in urban parks in summer and winter. *Build. Environ.* 164, 106364. <https://doi.org/10.1016/j.buildenv.2019.106364>.
- Chen, X., Gao, L.X., Xue, P.N., Du, J., Liu, J., 2020. Investigation of outdoor thermal sensation and comfort evaluation methods in severe cold area. *Sci. Total Environ.* 749, <https://doi.org/10.1016/j.scitotenv.2020.141520>.
- Cheng, V., Ng, E., Chan, C., Givoni, B., 2012. Outdoor thermal comfort study in a sub-tropical climate: a longitudinal study based in Hong Kong. *Int. J. Biometeorol.* 56 (1), 43–56. <https://doi.org/10.1007/s00484-010-0396-z>.
- Chiang, Y.-C., Liu, H.-H., Li, D., Ho, L.-C., 2023. Quantification through deep learning of sky view factor and greenery on urban streets during hot and cool seasons. *Landsc. Urban Plan.* 232, 104679. <https://doi.org/10.1016/j.landurbplan.2022.104679>.
- China Meteorological Administration (CMA), 2025. Retrieved from <http://data.cma.cn/>.
- Choropoulous, K., Kamoutsis, A., Matsoukis, A., Manoli, E., 2012. An artificial neural network model application for the estimation of thermal comfort conditions in mountainous regions. *Greece. Atmosfera* 25 (2), 171–181.
- Coccolo, S., Kampf, J., Scartezzini, J.L., Pearlmutter, D., 2016. Outdoor human comfort and thermal stress: A comprehensive review on models and standards. *Urban Clim.* 18, 33–57. <https://doi.org/10.1016/j.uclim.2016.08.004>.
- Currie, J., Deschênes, O., 2016. Children and climate change: introducing the issue. *Futur. Child.* 3–9. <https://doi.org/10.1353/foc.2016.0000>.
- Dadvand, P., Bartoll, X., Basagana, X., Dalmau-Bueno, A., Martínez, D., Ambros, A., Cirach, M., Triguero-Mas, M., Gascon, M., Borrell, C., 2016. Green spaces and general health: roles of mental health status, social support, and physical activity. *Environ. Int.* 91, 161–167. <https://doi.org/10.1016/j.envint.2016.02.029>.
- de Freitas, C.R., Grigorieva, E.A., 2017. A comparison and appraisal of a comprehensive range of human thermal climate indices. *Int. J. Biometeorol.* 61 (3), 487–512. <https://doi.org/10.1007/s00484-016-1228-6>.
- de Oña, J., Garrido, C., 2014. Extracting the contribution of independent variables in neural network models: a new approach to handle instability. *Neural Comput. & Applic.* 25 (3), 859–869. <https://doi.org/10.1007/s00521-014-1573-5>.
- Deng, Z., Chen, Q., 2018. Artificial neural network models using thermal sensations and occupants' behavior for predicting thermal comfort. *Energ. Buildin.* 174, 587–602. <https://doi.org/10.1016/j.enbuild.2018.06.060>.
- Elnabawi, M.H., Hamza, N., Dudek, S., 2016. Thermal perception of outdoor urban spaces in the hot arid region of Cairo, Egypt. *Sustain. Cities Soc.* 22, 136–145. <https://doi.org/10.1016/j.scs.2016.02.005>.
- Eslamirad, N., Malekpour Kolbadinejad, S., Mahdavinejad, M., Mehranrad, M., 2020. Thermal comfort prediction by applying supervised machine learning in green sidewalks of Tehran. *Smart Sustain. Built Environ.* 9 (4), 361–374. <https://doi.org/10.1108/SASBE-03-2019-0028>.
- Fanger, P.O., 1970. *Thermal Comfort: Analysis and Applications in Environmental Engineering*.
- Geng, Y., Hong, B., Du, M., Yuan, T., Wang, Y., 2021. Combined effects of visual-acoustic-thermal comfort in campus open spaces: A pilot study in China's cold region. *Build. Environ.* 108658. <https://doi.org/10.1016/j.buildenv.2021.108658>.
- Graupe, D., 2013. *Principles of Artificial Neural Networks*, Vol. 7. World Scientific.
- Hadianpour, M., Mahdavinejad, M., Bemanian, M., Nasrollahi, F., 2018. Seasonal differences of subjective thermal sensation and neutral temperature in an outdoor shaded space in Tehran, Iran. *Sustain. Cities Soc.* 39, 751–764. <https://doi.org/10.1016/j.scs.2018.03.003>.
- Hamby, D.M., 1994. A review of techniques for parameter sensitivity analysis of environmental models. *Environ. Monit. Assess.* 32 (2), 135–154. <https://doi.org/10.1007/BF00547132>.
- Havenith, G., 2007. Metabolic rate and clothing insulation data of children and adolescents during various school activities. *Ergonomics* 50 (10), 1689–1701. <https://doi.org/10.1080/00140130701587574>.
- He, X., An, L., Hong, B., Huang, B., Cui, X., 2020. Cross-cultural differences in thermal comfort in campus open spaces: A longitudinal field survey in China's cold region. *Build. Environ.* 172. <https://doi.org/10.1016/j.buildenv.2020.106739>.
- He, X., Shao, L., Tang, Y., Wu, S., 2023. Improving children's outdoor thermal comfort: A field study in China's severely cold regions. *Urban Clim.* 51, 101620. <https://doi.org/10.1016/j.uclim.2023.101620>.
- Hecht, N., 1989. Theory of the backpropagation neural network. In: Paper Presented at the International 1989 Joint Conference on Neural Networks.
- Hecht-Nielsen, R., 1987. *Kolmogorov's Mapping Neural Network Existence Theorem*.
- Hirst, J.D., Sternberg, M.J., 1992. Prediction of structural and functional features of protein and nucleic acid sequences by artificial neural networks. *Biochemistry* 31 (32), 7211–7218. <https://doi.org/10.1021/bi00147a001>.
- Höppe, P., 1999. The physiological equivalent temperature - A universal index for the biometeorological assessment of the thermal environment. *Int. J. Biometeorol.* 43 (2), 71–75. <https://doi.org/10.1007/s004840050118>.
- Huang, B., Hong, B., Tian, Y., Yuan, T., Su, M., 2021. Outdoor thermal benchmarks and thermal safety for children: A study in China's cold region. *Sci. Total Environ.* 787, 147603. <https://doi.org/10.1016/j.scitotenv.2021.147603>.
- ISO International Standard 9920, 2007. *Ergonomics of the Thermal Environment: Estimation of Thermal Insulation and Water Vapour Resistance of a Clothing Ensemble*. In: International Standard Origination, Geneva.
- Javadi, R., Nasrollahi, N., 2021. Urban green space and health: the role of thermal comfort on the health benefits from the urban green space; a review study. *Build. Environ.* 202. <https://doi.org/10.1016/j.enbuild.2021.108039>.
- Jendritzky, G., de Dear, R., Havenith, G., 2012. UTCI-why another thermal index? *Int. J. Biometeorol.* 56 (3), 421–428. <https://doi.org/10.1007/s00484-011-0513-7>.
- Kalogirou, S.A., 2000. Applications of artificial neural-networks for energy systems. *Appl. Energy* 67 (1), 17–35. [https://doi.org/10.1016/S0306-2619\(00\)00005-2](https://doi.org/10.1016/S0306-2619(00)00005-2).
- Kariminia, S., Shamshirband, S., Motamed, S., Hashim, R., Roy, C., 2016. A systematic extreme learning machine approach to analyze visitors' thermal comfort at a public urban space. *Renew. Sust. Energ. Rev.* 58, 751–760. <https://doi.org/10.1016/j.rser.2015.12.321>.
- Kennedy, E., Olsen, H., Vanos, J., Vecellio, D.J., Desat, M., Richters, K., Rutledge, A., Richardson, G.R.A., 2021. Reimagining spaces where children play: developing guidance for thermally comfortable playgrounds in Canada. *Can. J. Public Health* 112 (4), 706–713. <https://doi.org/10.17269/s41997-021-00522-7>.
- Khairunniza-Bejo, S., Mustaffha, S., Ismail, W.I.W., 2014. Application of artificial neural network in predicting crop yield: A review. *J. Food Sci. Eng. Anal.* 4 (1), 1.

- Krüger, E.L., Rossi, F.A., 2011. Effect of personal and microclimatic variables on observed thermal sensation from a field study in southern Brazil. *Build. Environ.* 46 (3), 690–697. <https://doi.org/10.1016/j.buildenv.2010.09.013>.
- Krüger, E.L., Tamura, C.A., Bröde, P., Schweikert, M., Wagner, A., 2017. Short- and long-term acclimatization in outdoor spaces: exposure time, seasonal and heatwave adaptation effects. *Build. Environ.* 116, 17–29. <https://doi.org/10.1016/j.buildenv.2017.02.001>.
- Lai, D., Guo, D., Hou, Y., Lin, C., Chen, Q., 2014a. Studies of outdoor thermal comfort in northern China. *Build. Environ.* 77, 110–118. <https://doi.org/10.1016/j.buildenv.2014.03.026>.
- Lai, D., Zhou, C., Huang, J., Jiang, Y., Long, Z., Chen, Q., 2014b. Outdoor space quality: A field study in an urban residential community in Central China. *Energ. Buildin.* 68, 713–720. <https://doi.org/10.1016/j.enbuild.2013.02.051>.
- Lam, C.K.C., Hang, J., Zhang, D., Wang, Q., Ren, M., Huang, C., 2021. Effects of short-term physiological and psychological adaptation on summer thermal comfort of outdoor exercising people in China. *Build. Environ.* 198. <https://doi.org/10.1016/j.buildenv.2021.107877>.
- Lam, C.K.C., Shooshtarian, S., Kenawy, I., 2023. Assessment of urban physical features on summer thermal perceptions using the local climate zone classification. *Build. Environ.* 236, 110265. <https://doi.org/10.1016/j.buildenv.2023.110265>.
- Lau, K.K.L., Choi, C.Y., 2021. The Influence of Perceived Environmental Quality on Thermal Comfort in an Outdoor Urban Environment during Hot Summer.
- Li, Y., Nian, X., Gu, C., Deng, P., He, S., Hong, B., 2024. Assessing children's outdoor thermal comfort with facial expression recognition: An efficient approach using machine learning. *Build. Environ.* 258, 111556. <https://doi.org/10.1016/j.buildenv.2024.111556>.
- Lin, T.-P., Matzarakis, A., Hwang, R.-L., 2010. Shading effect on long-term outdoor thermal comfort. *Build. Environ.* 45 (1), 213–221. <https://doi.org/10.1016/j.buildenv.2009.06.002>.
- Liu, K.X., Nie, T., Liu, W., Liu, Y.Q., Lai, D.Y., 2020. A machine learning approach to predict outdoor thermal comfort using local skin temperatures. *Sustain. Cities Soc.* 59. <https://doi.org/10.1016/j.scs.2020.102216>.
- Maas, J., Verheij, R.A., de Vries, S., Spreeuwenberg, P., Schellevis, F.G., Groenewegen, P.P., 2009. Morbidity is related to a green living environment. *J. Epidemiol. Community Health* 63 (12), 967–973. <https://doi.org/10.1136/jech.2008.079038>.
- Maier, H.R., Dandy, G.C., 2000. Neural networks for the prediction and forecasting of water resources variables: a review of modelling issues and applications. *Environ. Model Softw.* 15 (1), 101–124. [https://doi.org/10.1016/S1364-8152\(99\)00007-9](https://doi.org/10.1016/S1364-8152(99)00007-9).
- Matzarakis, A., Mayer, H., 1996. Another kind of environmental stress: thermal stress.
- Mba, L., Meukam, P., Kemajou, A., 2016. Application of artificial neural network for predicting hourly indoor air temperature and relative humidity in modern building in humid region. *Energ. Buildin.* 121, 32–42. <https://doi.org/10.1016/j.enbuild.2016.03.046>.
- Mladenović, I., Sokolov-Mladenović, S., Milovanović, M., Marković, D., Simeunović, N., 2016. Management and estimation of thermal comfort, carbon dioxide emission and economic growth by support vector machine. *Renew. Sust. Energ. Rev.* 64, 466–476. <https://doi.org/10.1016/j.rser.2016.06.034>.
- Mors, S.T., Hensen, J.L.M., Loomans, M.G.L.C., Boerstra, A.C., 2011. Adaptive thermal comfort in primary school classrooms: creating and validating PMV-based comfort charts. *Build. Environ.* 46 (12), 2454–2461. <https://doi.org/10.1016/j.buildenv.2011.05.025>.
- Nikolopoulou, M., Steemers, K., 2003. Thermal comfort and psychological adaptation as a guide for designing urban spaces. *Energ. Buildin.* 35 (1), 95–101. [https://doi.org/10.1016/S0378-7788\(02\)00084-1](https://doi.org/10.1016/S0378-7788(02)00084-1).
- Omar, N., Johari, Z.A., Smith, M., 2017. Predicting fraudulent financial reporting using artificial neural network. *J. Finan. Crime* 24 (2), 362–387. <https://doi.org/10.1108/JFC-11-2015-0061>.
- Pentó, K., 2016. The methods of extracting the contribution of variables in artificial neural network models – comparison of inherent instability. *Comput. Electron. Agric.* 127, 141–146. <https://doi.org/10.1016/j.compag.2016.06.010>.
- Qin, H., Cheng, X., Han, G., Wang, Y., Deng, J., Yang, Y., 2021. How thermal conditions affect the spatial-temporal distribution of visitors in urban parks: A case study in Chongqing, China. *Urban For. Urban Green.* 66. <https://doi.org/10.1016/j.ufug.2021.127393>.
- Ruiz, M.A., Correa, E.N., 2015. Adaptive model for outdoor thermal comfort assessment in an oasis city of arid climate. *Build. Environ.* 85, 40–51. <https://doi.org/10.1016/j.buildenv.2014.11.018>.
- Salata, F., Golasi, I., de Lieto Vollaro, R., de Lieto Vollaro, A., 2016. Outdoor thermal comfort in the Mediterranean area. A transversal study in Rome, Italy. *Build. Environ.* 96, 46–61. <https://doi.org/10.1016/j.buildenv.2015.11.023>.
- Seltenrich, N., 2015. Just what the doctor ordered: using parks to improve children's health. *Environ. Health Perspect.* <https://doi.org/10.1289/ehp.123-A254>.
- Shahzad, S., Brennan, J., Theodossopoulos, D., Calautit, J.K., Hughes, B.R., 2018. Does a neutral thermal sensation determine thermal comfort? *Build. Serv. Eng. Res. Technol.* 39 (2), 183–195. <https://doi.org/10.1177/0143624418754498>.
- Shan, C., Hu, J., Wu, J., Zhang, A., Ding, G., Xu, L.X., 2020. Towards non-intrusive and high accuracy prediction of personal thermal comfort using a few sensitive physiological parameters. *Energ. Buildin.* 207, 109594. <https://doi.org/10.1016/j.enbuild.2019.109594>.
- Shao, L., He, X., Tang, Y., Wu, S., 2022. Outdoor cold stress and cold risk for children during winter: A study in China's severe cold regions. *Buildings* 12 (7), 936. <https://doi.org/10.3390/buildings12070936>.
- Shooshtarian, S., 2015. Socio-economic factors for the perception of outdoor thermal environments: towards climate-sensitive Urban Design. *Global Built Environ. Review* 9 (3).
- Su, Y., Wang, C., Li, Z., Meng, Q., Gong, A., Wu, Z., Zhao, Q., 2024. Summer outdoor thermal comfort assessment in city squares—A case study of cold dry winter, hot summer climate zone. *Sustain. Cities Soc.* 101, 105062. <https://doi.org/10.1016/j.scs.2023.105062>.
- Tyrväinen, L., Ojala, A., Korpela, K., Lankki, T., Tsunetsugu, Y., Kagawa, T., 2014. The influence of urban green environments on stress relief measures: A field experiment. *J. Environ. Psychol.* 38, 1–9. <https://doi.org/10.1016/j.jenp.2013.12.005>.
- Vanaken, G.J., Danckaerts, M., 2018. Impact of green space exposure on children's and adolescents' mental health: A systematic review. *Int. J. Environ. Res. Public Health* 15 (12), 2668. <https://doi.org/10.3390/ijerph15122668>.
- Vanos, J.K., 2015. Children's health and vulnerability in outdoor microclimates: A comprehensive review. *Environ. Int.* 76, 1–15. <https://doi.org/10.1016/j.envint.2014.11.016>.
- Villadiego, K., Velay-Dabat, M.A., 2014. Outdoor thermal comfort in a hot and humid climate of Colombia: A field study in Barranquilla. *Build. Environ.* 75, 142–152. <https://doi.org/10.1016/j.buildenv.2014.01.017>.
- von Grabe, J., 2016. Potential of artificial neural networks to predict thermal sensation votes. *Appl. Energy* 161, 412–424. <https://doi.org/10.1016/j.apenergy.2015.10.061>.
- Wardah, W., Khan, M.G., Sharma, A., Rashid, M.A., 2019. Protein secondary structure prediction using neural networks and deep learning: A review. *Comput. Biol. Chem.* 81, 1–8. <https://doi.org/10.1016/j.compbiochem.2019.107093>.
- WHO, 2020a. Children: New Threats to Health. Retrieved from. <https://www.who.int/news-room/fact-sheets/detail/children-new-threats-to-health>.
- WHO, 2020b. Urban Green Spaces and Health. Retrieved from. <https://iris.who.int/handle/10665/345751>.
- Xu, Z., Sheffield, P.E., Hu, W., Su, H., Yu, W., Qi, X., Tong, S., 2012. Climate change and children's health—A call for research on what works to protect children. *Int. J. Environ. Res. Public Health* 9 (9), 3298–3316. <https://doi.org/10.3390/ijerph9093298>.
- Yang, C., Prasher, S.O., Landry, J., DiTommaso, A., 2000. Application of artificial neural networks in image recognition and classification of crop and weeds. *Can. Agric. Eng.* 42 (3), 147–152. [https://doi.org/10.1016/S0960-8524\(99\)00141-8](https://doi.org/10.1016/S0960-8524(99)00141-8).
- Yang, W., Wong, N.H., Zhang, G., 2013. A comparative analysis of human thermal conditions in outdoor urban spaces in the summer season in Singapore and Changsha, China. *Int. J. Biometeorol.* 57 (6), 895–907. <https://doi.org/10.1007/s00484-012-0616-9>.

- Yang, Y., Lyu, J., Du, H., Lian, Z., Liu, W., Duanmu, L., Zhai, Y., Cao, B., Zhang, Y., Zhou, X., Wang, Z., Zhang, X., Wang, F., 2024. Main effects and interactions of multiple key factors related to thermal perception. *Sci. Total Environ.* 918, 170683. <https://doi.org/10.1016/j.scitotenv.2024.170683>.
- Yin, J.F., Zheng, Y.F., Wu, R.J., Tan, J.G., Ye, D.X., Wang, W., 2012. An analysis of influential factors on outdoor thermal comfort in summer. *Int. J. Biometeorol.* 56 (5), 941–948. <https://doi.org/10.1007/s00484-011-0503-9>.
- Zhang, Y., Zhou, X., Zheng, Z., Oladokun, M.O., Fang, Z., 2020. Experimental investigation into the effects of different metabolic rates of body movement on thermal comfort. *Build. Environ.* 168, 106489. <https://doi.org/10.1016/j.buildenv.2019.106489>.
- Zhang, T., Su, M., Hong, B., Wang, C., Li, K., 2021. Interaction of emotional regulation and outdoor thermal perception: A pilot study in a cold region of China. *Build. Environ.* 198. <https://doi.org/10.1016/j.buildenv.2021.107870>.
- Zhao, L.J., Zhou, X.Q., Li, L., He, S.Q., Chen, R.C., 2016. Study on outdoor thermal comfort on a campus in a subtropical urban area in summer. *Sustain. Cities Soc.* 22, 164–170. <https://doi.org/10.1016/j.scs.2016.02.009>.
- Zheng, P., Yao, R., Toftum, J., Liu, S., Kalmár, F., Li, B., 2024. Evaluation methods and factors influencing the thermal comfort of children-a comprehensive literature review. *J. Build. Eng.* 110063.